Search for the neutral Higgs bosons of the minimal supersymmetric standard model from Z^0 decays

L3 Collaboration

B. Adeva [a], O. Adriani [b], M. Aguilar-Benitez [c], H. Akbari [d], J. Alcaraz [c], A. Aloisio [e], G. Alverson [f], M.G. Alviggi [e], Q. An [g], H. Anderhub [h], A.L. Anderson [i], V.P. Andreev [j], T. Angelov [i], L. Antonov [k], D. Antreasyan [ℓ], P. Arce [c], A. Arefiev [m], T. Azemoon [n], T. Aziz [o], P.V.K.S. Baba [g], P. Bagnaia [p], J.A. Bakken [q], L. Baksay [r], R.C. Ball [n], S. Banerjee [o,g], J. Bao [d], L. Barone [p], A. Bay [s], U. Becker [i], J. Behrens [h], S. Beingessner [t], Gy.L. Bencze [u], J. Berdugo [c], P. Berges [i], B. Bertucci [p], B.L. Betev [k], A. Biland [h], R. Bizzarri [p], J.J. Blaising [t], P. Blömeke [v], B. Blumenfeld [d], G.J. Bobbink [w], M. Bocciolini [b], W. Böhlen [x], A. Böhm [v], T. Böhringer [y], B. Borgia [p], D. Bourilkov [k], M. Bourquin [s], D. Boutigny [t], J.G. Branson [z], I.C. Brock [aa], F. Bruyant [a], C. Buisson [ab], A. Bujak [ac], J.D. Burger [i], J.P. Burq [ab], J. Busenitz [ad], X.D. Cai [g], C. Camps [v], M. Capell [n], F. Carbonara [e], F. Carminati [b], A.M. Cartacci [b], M. Cerrada [c], F. Cesaroni [p], Y.H. Chang [i], U.K. Chaturvedi [g], M. Chemarin [ab], A. Chen [ae], C. Chen [af], G.M. Chen [af], H.F. Chen [ag], H.S. Chen [af], M. Chen [i], M.C. Chen [ah], M.L. Chen [n], G. Chiefari [e], C.Y. Chien [d], C. Civinini [b], I. Clare [i], R. Clare [i], G. Coignet [t], N. Colino [a], V. Commichau [v], G. Conforto [b], A. Contin [a], F. Crijns [w], X.Y. Cui [g], T.S. Dai [i], R. D'Alessandro [b], R. de Asmundis [e], A. Degré [a,t], K. Deiters [a,ai], E. Dénes [u], P. Denes [q], F. DeNotaristefani [p], M. Dhina [h], D. DiBitonto [ad], M. Diemoz [p], F. Diez-Hedo [a], H.R. Dimitrov [k], C. Dionisi [p], F. Dittus [ah], R. Dolin [i], E. Drago [e], T. Driever [w], D. Duchesneau [s], P. Duinker [w,a], I. Duran [a,c], H. El Mamouni [ab], A. Engler [aa], F.J. Eppling [i], F.C. Erné [w], P. Extermann [s], R. Fabbretti [h], G. Faber [i], S. Falciano [p], Q. Fan [g,af], S.J. Fan [aj], M. Fabre [h], J. Fay [ab], J. Fehlmann [h], H. Fenker [f], T. Ferguson [aa], G. Fernandez [c], F. Ferroni [p,a], H. Fesefeldt [v], J. Field [s], G. Finocchiaro [p], P.H. Fisher [d], G. Forconi [s], T. Foreman [w], K. Freudenreich [h], W. Friebel [ai], M. Fukushima [i], M. Gailloud [y], Yu. Galaktionov [m], E. Gallo [b], S.N. Ganguli [o], P. Garcia-Abia [c], S.S. Gau [ae], S. Gentile [p], M. Glaubman [f], S. Goldfarb [n], Z.F. Gong [g,ag], E. Gonzalez [c], A. Gordeev [m], P. Göttlicher [v], D. Goujon [s], G. Gratta [ah], C. Grinnell [i], M. Gruenewald [ah], M. Guanziroli [g], A. Gurtu [o], H.R. Gustafson [n], L.J. Gutay [ac], H. Haan [v], S. Hancke [v], K. Hangarter [v], M. Harris [a], A. Hasan [g], C.F. He [aj], T. Hebbeker [v], M. Hebert [z], G. Herten [i], U. Herten [v], A. Hervé [a], K. Hilgers [v], H. Hofer [h], H. Hoorani [g], L.S. Hsu [ae], G. Hu [g], G.Q. Hu [aj], B. Ille [ab], M.M. Ilyas [g], V. Innocente [e,a], E. Isiksal [h], E. Jagel [g], B.N. Jin [af], L.W. Jones [n], R.A. Khan [g], Yu. Kamyshkov [m], Y. Karyotakis [t,a], M. Kaur [g], S. Khokhar [g], V. Khoze [j], D. Kirkby [ah], W. Kittel [w], A. Klimentov [m], A.C. König [w], O. Kornadt [v], V. Koutsenko [m], R.W. Kraemer [aa], T. Kramer [i], V.R. Krastev [k], W. Krenz [v], J. Krizmanic [d], A. Kuhn [x], K.S. Kumar [ak], V. Kumar [g], A. Kunin [m], A.van Laak [v], V. Lalieu [s], G. Landi [b], K. Lanius [a], D. Lanske [v], S. Lanzano [e], P. Lebrun [ab], P. Lecomte [h], P. Lecoq [a], P.Le Coultre [h], I. Leedom [f], J.M. Le Goff [a], L. Leistam [a], R. Leiste [ai], M. Lenti [b], J. Lettry [h], P.M. Levchenko [j], X. Leytens [w], C. Li [ag], H.T. Li [af], J.F. Li [g], L. Li [h], P.J. Li [aj], Q. Li [g], X.G. Li [af], J.Y. Liao [aj], Z.Y. Lin [ag], F.L. Linde [aa], D. Linnhofer [a], R. Liu [g], Y. Liu [g], W. Lohmann [ai], S. Lökös [r], E. Longo [p], Y.S. Lu [af], J.M. Lubbers [w], K. Lübelsmeyer [v], C. Luci [a], D. Luckey [ℓ,i], L. Ludovici [p], X. Lue [h], L. Luminari [p], W.G. Ma [ag], M. MacDermott [h], R. Magahiz [r], M. Maire [t], P.K. Malhotra [o],

0370-2693/90/$ 03.50 © 1990 – Elsevier Science Publishers B.V. (North-Holland)

R. Malik [g], A. Malinin [m], C. Maña [c], D.N. Mao [n], Y.F. Mao [af], M. Maolinbay [h], P. Marchesini [g], A. Marchionni [b], J.P. Martin [ab], L. Martinez [a], F. Marzano [p], G.G.G. Massaro [w], T. Matsuda [i], K. Mazumdar [o], P. McBride [ak], T. McMahon [ac], D. McNally [h], Th. Meinholz [v], M. Merk [w], L. Merola [e], M. Meschini [b], W.J. Metzger [w], Y. Mi [g], M. Micke [v], U. Micke [v], G.B. Mills [n], Y. Mir [g], G. Mirabelli [p], J. Mnich [v], M. Möller [v], B. Monteleoni [b], G. Morand [s], R. Morand [t], S. Morganti [p], V. Morgunov [m], R. Mount [ah], E. Nagy [u], M. Napolitano [e], H. Newman [ah], M.A. Niaz [g], L. Niessen [v], D. Pandoulas [v], G. Passaleva [b], G. Paternoster [e], S. Patricelli [e], Y.J. Pei [v], D. Perret-Gallix [t], J. Perrier [s], A. Pevsner [d], M. Pieri [b], P.A. Piroué [q], V. Plyaskin [m], M. Pohl [h], V. Pojidaev [m], N. Produit [s], J.M. Qian [i, g], K.N. Qureshi [g], R. Raghavan [o], G. Rahal-Callot [h], P. Razis [h], K. Read [q], D. Ren [h], Z. Ren [g], S. Reucroft [f], O. Rind [n], C. Rippich [aa], H.A. Rizvi [g], B.P. Roe [n], M. Röhner [v], S. Röhner [v], U. Roeser [ai], Th. Rombach [v], L. Romero [c], J. Rose [v], S. Rosier-Lees [t], R. Rosmalen [w], Ph. Rosselet [y], J.A. Rubio [a, c], W. Ruckstuhl [s], H. Rykaczewski [h], M. Sachwitz [ai], J. Salicio [a, c], J.M. Salicio [c], G. Sartorelli [ℓ, g], G. Sauvage [t], A. Savin [m], V. Schegelsky [j], D. Schmitz [v], P. Schmitz [v], M. Schneegans [t], M. Schöntag [v], H. Schopper [aℓ], D.J. Schotanus [w], H.J. Schreiber [ai], R. Schulte [v], S. Schulte [v], K. Schultze [v], J. Schütte [ak], J. Schwenke [v], G. Schwering [v], C. Sciacca [e], I. Scott [ak], R. Sehgal [g], P.G. Seiler [h], J.C. Sens [w], I. Sheer [z], V. Shevchenko [m], S. Shevchenko [m], X.R. Shi [aa], K. Shmakov [m], V. Shoutko [m], E. Shumilov [m], N. Smirnov [j], A. Sopczak [ah, z], C. Spartiotis [d], T. Spickermann [v], B. Spiess [x], P. Spillantini [b], R. Starosta [v], M. Steuer [ℓ, i], D.P. Stickland [q], B. Stöhr [h], H. Stone [s], K. Strauch [ak], B.C. Stringfellow [ac], K. Sudhakar [o, v], G. Sultanov [a], R.L. Sumner [q], L.Z. Sun [ag], H. Suter [h], R.B. Sutton [aa], J.D. Swain [g], A.A. Syed [g], X.W. Tang [af], E. Tarkovsky [m], L. Taylor [f], E. Thomas [g], C. Timmermans [w], Samuel C.C. Ting [i], S.M. Ting [i], Y.P. Tong [ae], F. Tonisch [ai], M. Tonutti [v], S.C. Tonwar [o], J. Tòth [u], G. Trowitzsch [ai], K.L. Tung [af], J. Ulbricht [x], L. Urbàn [u], U. Uwer [v], E. Valente [p], R.T. Van de Walle [w], H. van der Graaf [w], I. Vetlitsky [m], G. Viertel [h], P. Vikas [g], U. Vikas [g], M. Vivargent [t, i], H. Vogel [aa], H. Vogt [ai], M. Vollmar [v], G. Von Dardel [a], I. Vorobiev [m], A.A. Vorobyov [j], An.A. Vorobyov [j], L. Vuilleumier [y], M. Wadhwa [g], W. Wallraff [v], C.R. Wang [ag], G.H. Wang [aa], J.H. Wang [af], Q.F. Wang [ak], X.L. Wang [ag], Y.F. Wang [b], Z. Wang [g], Z.M. Wang [g, ag], J. Weber [h], R. Weill [y], T.J. Wenaus [i], J. Wenninger [s], M. White [i], R. Wilhelm [w], C. Willmott [c], F. Wittgenstein [a], D. Wright [q], R.J. Wu [af], S.L. Wu [g], S.X. Wu [g], Y.G. Wu [af], B. Wysłouch [i], Y.D. Xu [af], Z.Z. Xu [ag], Z.L. Xue [aj], D.S. Yan [aj], B.Z. Yang [ag], C.G. Yang [af], G. Yang [g], K.S. Yang [af], Q.Y. Yang [af], Z.Q. Yang [aj], C.H. Ye [g], J.B. Ye [h], Q. Ye [g], S.C. Yeh [ae], Z.W. Yin [aj], J.M. You [g], C. Zaccardelli [ah], L. Zehnder [h], M. Zeng [g], Y. Zeng [v], D. Zhang [z], D.H. Zhang [w], Z.P. Zhang [ag], J.F. Zhou [v], R.Y. Zhu [ah], H.L. Zhuang [af] and A. Zichichi [a, g]

[a] *European Laboratory for Particle Physics, CERN, CH-1211 Geneva 23, Switzerland*
[b] *INFN – Sezione di Firenze and University of Firenze, I-50125 Florence, Italy*
[c] *Centro de Investigaciones Energeticas, Medioambientales y Tecnologicas, CIEMAT, E-28040 Madrid, Spain*
[d] *Johns Hopkins University, Baltimore, MD 21218, USA*
[e] *INFN – Sezione di Napoli and University of Naples, I-80125 Naples, Italy*
[f] *Northeastern University, Boston, MA 02115, USA*
[g] *World Laboratory, FBLJA Project, CH-1211 Geneva, Switzerland*
[h] *Eidgenössische Technische Hochschule, ETH Zürich, CH-8093 Zurich, Switzerland*
[i] *Massachusetts Institute of Technology, Cambridge, MA 02139, USA*
[j] *Leningrad Nuclear Physics Institute, SU-188 350 Gatchina, USSR*
[k] *Central Laboratory of Automation and Instrumentation, CLANP, Sofia, Bulgaria*
[ℓ] *INFN – Sezione di Bologna, I-40126 Bologna, Italy*
[m] *Institute of Theoretical and Experimental Physics, ITEP, SU-117 259 Moscow, USSR*
[n] *University of Michigan, Ann Arbor, MI 48109, USA*
[o] *Tata Institute of Fundamental Research, Bombay 400 005, India*
[p] *INFN – Sezione di Roma and University of Rome "La Sapienza", I-00185 Rome, Italy*

[q] Princeton University, Princeton, NJ 08544, USA
[r] Union College, Schenectady, NY 12308, USA
[s] University of Geneva, CH-1211 Geneva 4, Switzerland
[t] Laboratoire de Physique des Particules, LAPP, F-74519 Annecy-le-Vieux, France
[u] Central Research Institute for Physics of the Hungarian Academy of Sciences, H-1525 Budapest 114, Hungary
[v] I. Physikalisches Institut, RWTH, W-5100 Aachen, FRG[1]
and III. Physikalisches Institut, RWTH, W-5100 Aachen, FRG[1]
[w] National Institute for High Energy Physics, NIKHEF, NL-1009 DB Amsterdam, The Netherlands
and NIKHEF-H and University of Nijmegen, NL-6525 ED Nijmegen, The Netherlands
[x] Paul Scherrer Institut (PSI), Würenlingen, Switzerland
[y] University of Lausanne, CH-1015 Lausanne, Switzerland
[z] University of California, San Diego, CA 92182, USA
[aa] Carnegie Mellon University, Pittsburgh, PA 15213, USA
[ab] Institut de Physique Nucléaire de Lyon, IN2P3-CNRS/Université Claude Bernard, F-69622 Villeurbanne Cedex, France
[ac] Purdue University, West Lafayette, IN 47907, USA
[ad] University of Alabama, Tuscaloosa, AL 35486, USA
[ae] High Energy Physics Group, Taiwan, ROC
[af] Institute of High Energy Physics, IHEP, Beijing, P.R. China
[ag] Chinese University of Science and Technology, USTC, Hefei, Anhui 230 029, P.R. China
[ah] California Institute of Technology, Pasadena, CA 91125, USA
[ai] High Energy Physics Institute, O-1615 Zeuthen-Berlin, FRG
[aj] Shanghai Institute of Ceramics, SIC, Shanghai, P.R. China
[ak] Harvard University, Cambridge, MA 02139, USA
[al] University of Hamburg, W-2000 Hamburg, FRG

Received 28 August 1990

We present the results from a search for the light neutral scalar Higgs boson h^0 and the pseudoscalar Higgs boson A^0 of the minimal super-symmetric standard model. The analysis is based on a data sample corresponding to 71 000 hadronic Z^0 decays recorded with the L3 detector at LEP. No evidence for the existence of the neutral Higgs bosons h^0 and A^0 has been found. The region of h^0 and A^0 masses up to 41.5 GeV is excluded at 95% confidence level.

1. Introduction

Although the standard model [1] provides a precise description of existing data on electroweak interactions, the Higgs boson, an essential ingredient of the model, has remained undetected. The Higgs sector [2] is crucial to ensure the renormalizability of the theory and to give masses to the gauge bosons (Z^0, $W^{\pm}$). In the standard model one doublet of a complex Higgs field gives rise to a single physical Higgs boson, H^0_{SM}.

The standard model has several theoretical difficulties. For example, scalar particles receive divergent corrections to their masses (hierarchy problem). The minimal supersymmetric standard model [3] (MSSM) addresses this and other theoretical problems in a consistent manner [4]. While the standard model Higgs boson may have a mass as high as one TeV, the lightest MSSM Higgs boson h^0 is confined to have a mass lower than the mass of the gauge boson Z^0 [5].

In this paper, we present a search for the light neutral Higgs bosons of the MSSM. Previous results on this subject can be found in ref. [6].

[1] Supported by the German Bundesministerium für Forschung und Technologie.

2. The Higgs bosons h^0, A^0

In the MSSM two doublets of complex Higgs fields lead to five physical Higgs bosons [4]: two neutral scalars h^0, H^0 (*CP* even), one neutral pseudoscalar A^0 (*CP* odd), and two charged scalars H^+, H^-. At current LEP energies only the search for h^0 and A^0 is possible due to the following theoretical constraints [5]:

$$m_{h^0} < m_{Z^0}\,, \quad m_{h^0} < m_{A^0}\,,$$

$$m_{H^0} > m_{Z^0}\,, \quad m_{H^\pm} > m_{W^\pm}\,.$$

The masses and couplings of the Higgs bosons in this model are highly constrained and can be expressed in terms of two free parameters such as (m_{h^0}, m_{A^0}) or (m_{h^0}, $\tan\beta$), where $\tan\beta = v_2/v_1$ is the ratio of the vacuum expectation values of the two Higgs doublets. Therefore, for a given m_{h^0}, $\tan\beta$ is directly related to m_{A^0}. If the vacuum expectation v_2 becomes much larger than v_1 (i.e. $\tan\beta \gg 1$) then m_{A^0} decreases to be close to m_{h^0}. On the other hand, when the vacuum expectation values are nearly equal (i.e. $\tan\beta \to 1$) then m_{A^0} becomes large and the h^0 becomes essentially the Higgs boson from the standard model H^0_{SM}. In this analysis we restrict ourselves to the theoretically favoured case [7] $\tan\beta > 1$, where the constraint comes from recent limits on the mass of the top quark [8,9].

The lightest Higgs boson h^0 can be produced either through the Bjorken process [10]:

$$Z^0 \to h^0 Z^{0*}\,, \tag{1}$$

or in association with A^0:

$$Z^0 \to h^0 A^0\,. \tag{2}$$

The h^0ZZ coupling is proportional to $\sin(\alpha-\beta)$, where α is the mixing angle between the two neutral scalars, so that the partial width for process (1) becomes large as the production rate of process (2) decreases with decreasing $\cos^2(\alpha-\beta)$,

$$\sin^2(\alpha-\beta) = \frac{\Gamma(Z^0 \to h^0 Z^{0*})}{\gamma(Z^0 \to H^0_{SM} Z^{0*})}\,, \tag{3}$$

and thus limits on the mass of the standard model Higgs can be translated into restrictions on the masses of h^0 and A^0. Since there is no A^0ZZ coupling (A^0 *CP* odd), at the tree level the A^0 can only be produced in association with h^0. The partial width for process (2) is proportional [11] to $\cos^2(\alpha-\beta)$ where

$$\cos^2(\alpha-\beta) = \frac{m^2_{h^0}(m^2_{Z^0} - m^2_{h^0})}{m^2_{A^0}(m^2_{Z^0} + m^2_{A^0} - 2m^2_{h^0})}\,. \tag{4}$$

The production rate becomes maximal when $m_{A^0} \approx m_{h^0}$ ($\tan\beta$ large).

The Higgs boson decays predominantly into the most massive kinematically accessible particle pair. In the MSSM one Higgs doublet couples to the up-type fermions only while the other couples to down-type fermions. In the case where $\tan\beta > 1$ the decay to up-type fermions is suppressed [11]. The branching ratios within the MSSM [12,13] are used for calculating the branching ratios of the Higgs bosons h^0 and A^0. In this paper we present the search for reaction (2) by considering the 3 dominant decay channels from the pair production of the Higgs bosons h^0 and A^0:

$$h^0 \to b\bar{b}\,, \quad A^0 \to b\bar{b}\,,$$

$$h^0 \to \tau\bar{\tau}\,, \quad A^0 \to b\bar{b}\,,$$

$$h^0 \to \tau\bar{\tau}\,, \quad A^0 \to \tau\bar{\tau}\,.$$

The signatures and the search strategies for these three processes are quite different from each other and are described in the subsequent sections. We also give a limit on the process (1) by translating our standard model Higgs limits [14,15] to the MSSM.

3. The L3 detector

The L3 detector covers 99% of 4π [16]. The detector includes a central vertex chamber, a precise electromagnetic calorimeter composed of bismuth germanium oxide crystals, a uranium and brass hadron calorimeter with proportional wire chamber readout, a high accuracy muon chamber system, and a ring of scintillation trigger counters. These detectors are installed in a magnet with an inner diameter of 12 m. The magnet provides a uniform field of 0.5 T along the beam direction. The luminosity is measured with two small angle electromagnetic calorimeters.

The fine segmentation of the electromagnetic detector and the hadron calorimeter allows us to measure the axis of jets with an angular resolution of 2.5°, and to measure the total energy of hadronic events from Z^0 decay with a resolution of 10% [17].

Events are collected at center of mass energies $\sqrt{s} = 88.2$–94.2 GeV from the 1990 LEP running period. For the search in the dimuon data sample, we use the data from March to August corresponding to 71 000 hadronic events, which leads to the upper mass limit. The other analysis results are based on data collected from March to July, which corresponds to 55 000 hadronic events. The simulated distributions in the cut quantities and in event shape variables agree very closely with the corresponding measured distributions [18].

4. Search for $h^0A^0 \to b\bar{b}b\bar{b}$

The signature of the decay channel where both Higgs bosons decay to $b\bar{b}$ quarks is a hadronic 4-jet event.

The primary trigger for hadronic events requires a total energy of 15 GeV in the central region of the calorimeters (polar angle region $|\cos\theta| < 0.74$), or 20 GeV in the entire detector. This trigger is in a logical OR with a trigger using the barrel scintillation counters and with a charged track trigger. The total trigger efficiency for accepted events of types $e^+e^- \to q\bar{q}$ and $e^+e^- \to h^0A^0 \to b\bar{b}b\bar{b}$ exceeds 99%.

Hadronic events were generated by the parton shower program JETSET 7.2 [19] with $\Lambda_{LL} = 290$ MeV and with string fragmentation. To simulate the gluon radiation and fragmentation of the b quarks from the Higgs decays, the same program has been used. The generated events were passed through the L3 detector simulation [20] which includes the effects of energy loss, multiple scattering, interactions and decays in the detector materials and beam pipe.

The event selection is based on the energy measured in the electromagnetic and hadron calorimeters:

(1) $0.6 < \frac{E_{vis}}{\sqrt{s}} < 1.4$,

(2) $\frac{|E_{\parallel}|}{E_{vis}} < 0.40$, $\frac{E_{\perp}}{E_{vis}} < 0.40$

(3) $N_{cluster} \geqslant 12$,

where E_{vis} is the total energy observed in the detector, $E_{\parallel}$ is the energy imbalance along the beam direction, and $E_{\perp}$ is the transverse energy imbalance. Neighbouring calorimetric hits which are most likely to be produced by the same particle are grouped into clusters. Thus the cut on the number of clusters rejects low multiplicity events ($Z^0 \to e^+e^-$, $\mu^+\mu^-$, $\tau^+\tau^-$). Cuts (1)–(3) select 99% of $e^+e^- \to h^0A^0 \to b\bar{b}b\bar{b}$ events.

Jets are reconstructed out of clusters in the calorimeters by using an invariant mass jet algorithm [21]. First the energy of each cluster is scaled by $\sqrt{s}/E_{vis}$. For each pair of clusters i and j the scaled invariant mass squared

$$y_{ij} = 2E_iE_j/s \cdot (1 - \cos\theta_{ij})$$

is then evaluated. E_i and E_j are the cluster energies and θ_{ij} is the angle between clusters i and j. The cluster pair for which y_{ij} is smallest is replaced by a pseudocluster k. This procedure is repeated until all scaled invariant masses squared, y_{ij}, exceeds the jet resolution parameter y_{cut}. The remaining pseudoclusters are called jets. Using this recombination scheme there is close agreement between jet rates at the parton level, the rates after hadronization, and the rates after reconstruction in the L3 detector [9,22]. We require that exactly four jets remain after this procedure for a jet resolution parameter $y_{cut} = 0.06$. We find a 4-jet rate of 0.57% in the data and a 4-jet rate of 0.42% in the simulation of $e^+e^- \to$ hadrons, where the difference reflects the limited precision of the parton shower Monte Carlo and the uncertainty in the fragmentation.

The Monte Carlo simulations have been performed at 21 h^0, A^0 mass combinations within the range of 22 GeV $\leqslant m_{h^0} \leqslant m_{A^0} \leqslant 42$ GeV. We choose the jet–jet combination with the minimal $\Delta m^2 = (m_1 - m_{h^0})^2 + (m_2 - m_{A^0})^2$, where m_1 and m_2 ($m_1 < m_2$) are the reconstructed invariant masses, out of the three possible combinations. We then reconstruct the kinematics of the Higgs bosons candidates. The remainder of the cuts are

(4) $N_{jet} = 4$ for jet resolution parameter $y_{cut} = 0.06$,

(5) $\cos\Theta_{production} < 0.4$,

(6) $\Delta m^2 < 22$ GeV^2,

(7) $|\Theta_{meas.opening} - \Theta_{exp.opening}(m_{h^0}, m_{A^0})| \leqslant 20^0$,

(8) $\cos\Theta_{decay} < 0.6$,

where $\Theta_{production}$ is the production angle, $\Theta_{opening}$ is the opening angle between jets belonging to the two Higgs candidates, and Θ_{decay} is the angle between the reconstructed Higgs direction and the jet directions in the restframe of the Higgs. The cut imposed on the production angles $\Theta_{production}$ of both Higgs bosons is shown in fig. 1. Since the event kinematics depend on the mass pair (m_{h^0}, m_{A^0}), the cut on the opening angles must also depend on (m_{h^0}, m_{A^0}). The acceptance for cuts (4)–(8) as a function of m_{h^0} and m_{A^0} is estimated by performing Monte Carlo simulations.

Fig. 2 shows the invariant mass distributions in the (m_1, m_2) plane for (a) data, and for (b) simulated $e^+e^- \to$ hadrons along with the Higgs signal for $m_{h^0} = m_{A^0} = 32$ GeV after cuts (1)–(5). We see the dominance of the simulated Higgs signal in the plot of the three possible jet–jet combinations.

The expected signal and the data are compared in the matrix of points in the (m_1, m_2) plane. To set a conservative limit we have reduced the number of expected events by 11% which accounts for systematic errors from the uncertainty in Monte Carlo statistics, event selection and production cross section. The (m_{h^0}, m_{A^0}) region A excluded at ≥95% confidence level is shown in fig. 3.

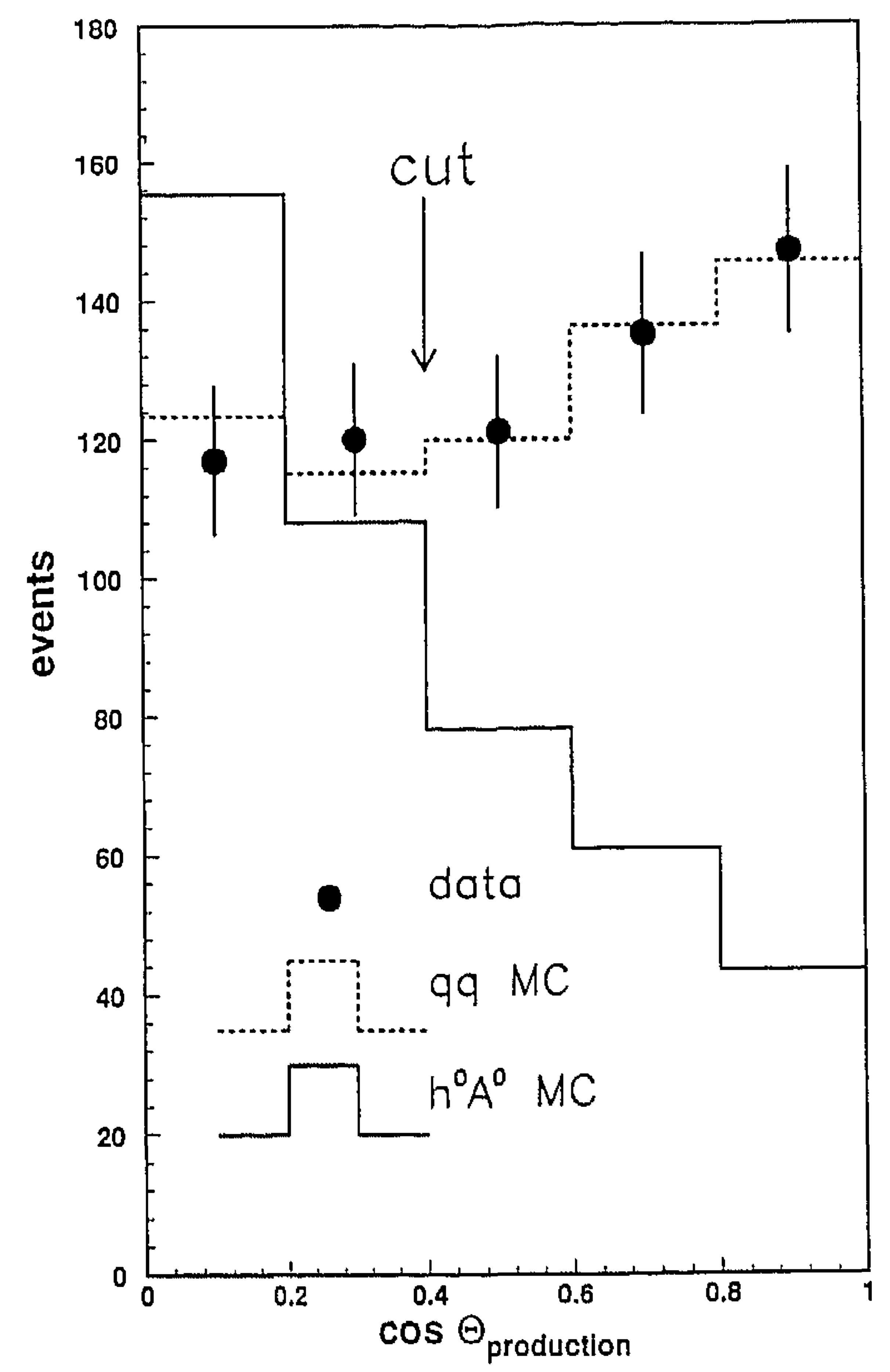

Fig. 1. Cosines of the reconstructed production angles of both Higgs candidates in the $h^0A^0 \to b\bar{b}b\bar{b}$ search. The jet–jet combination with smallest Δm is chosen. The simulated mass pair is $m_{h^0} = m_{A^0} = 32$ GeV. Cuts (1)–(4) are applied. The $q\bar{q}$ simulation is normalized to the number of data entries, whereas the signal simulation is normalized with respect to the expected cross section and branching ratio. Each event contributes twice.

An independent search in the $b\bar{b}b\bar{b}$ channel has been performed using hadron events with two muons. Triggers for inclusive dimuon events are described elsewhere [23]. They have a combined efficiency of greater than 99%. To search for $h^0A^0 \to b\bar{b}b\bar{b}$ decays in the inclusive dimuon data sample we employ the following selection criteria:

(1) The event is required to have two muon candidates, each of which must satisfy:

(a) $d_\perp < 3\sigma_{d_\perp}$ and $d_\parallel < 4\sigma_{d_\parallel}$,

(b) $E_\mu > 4$ GeV ,

(2) $N_{\mathrm{clusters}} > 50$,

(3) $\cos\Theta_{\mathrm{thrust}} < 0.65$,

(4) $E_{\mathrm{jet}_1} < 35$ GeV and $E_{\mathrm{jet}_2} < 26$ GeV ,

where $d_\perp$ ($d_\parallel$) is the distance of closest approach to the vertex in the transverse (longitudinal) plane, $\sigma_{d_\perp}$ ($\sigma_{d_\parallel}$) is the respective measurement error and E_μ is the measured energy of the muon. E_{jet_1} and E_{jet_2} are the energies of the two most energetic jets.

From Monte Carlo studies, we find that the acceptance of the h^0A^0 production after these cuts is 1.25% at $m_{h^0} = m_{A^0} = 40$ GeV and it slowly decreases as one moves away from this point in the (m_{h^0}, m_{A^0}) mass plane. We expect 4.7 events from the signal and 1.4 events from $e^+e^- \to$hadrons. No events survive the cuts in the entire mass region. The dominant error is due to Monte Carlo statistics. The total error in the region of high masses is estimated to be 19%. In fig. 3 the mass region B in the (m_{h^0}, m_{A^0}) plane is excluded by this part of the analysis at the 95% confidence level.

5. Search for $h^0A^0 \to \tau\bar{\tau}b\bar{b}$

The decay channel of $h^0 \to \tau\bar{\tau}$ and $A^0 \to b\bar{b}$ gives two taus in association with shower activities in the electromagnetic and hadron calorimeters. The search region for this process is

$$4\ \mathrm{GeV} < m_{h^0} < 30\ \mathrm{GeV}\ , \quad m_{A^0} > 10\ \mathrm{GeV}\ .$$

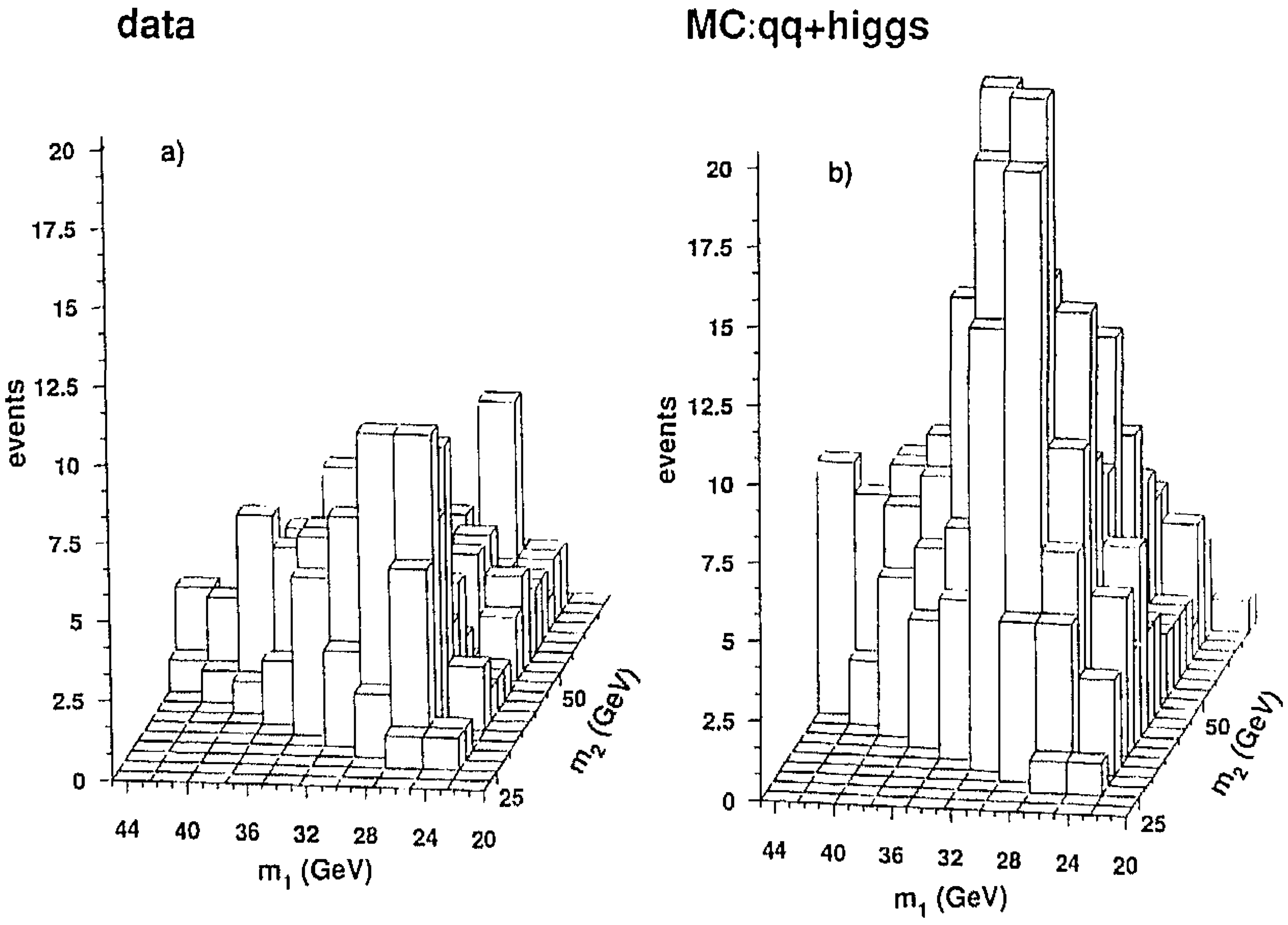

Fig. 2. m_1 (lower invariant mass) versus m_2 (higher invariant mass) for all three invariant mass combinations in the $h^0A^0 \to b\bar{b}b\bar{b}$ search. The plots (normalized as in fig. 1) show (a) data and (b) simulated signal ($m_{h^0} = m_{A^0} = 32$ GeV) plus background. Cuts (1)–(5) are applied.

The lower limits are due to the decay thresholds of h^0, A^0 to $\tau\bar{\tau}$ and $b\bar{b}$, respectively. The trigger efficiency for accepted events of this type exceeds 99%. We apply the following cuts:

(1) $40\ \text{GeV} < E_{\text{vis}} < 80\ \text{GeV}$,

(2) $\frac{|E_{\parallel}|}{E_{\text{vis}}} < 0.50 , \quad \frac{E_{\perp}}{E_{\text{vis}}} < 0.50$,

(3) $N_{\text{cluster}} \geq 12$.

Cut (1) takes into account the fact that in tau decays more energy escapes undetected compared to hadronic events. The acceptance for the generated $\tau\bar{\tau}\, b\bar{b}$ events after these cuts is about 85%.

Candidate $\tau\bar{\tau}\, b\bar{b}$ events are identified by dividing events into two hemispheres using the thrust axis as a normal vector and counting the number of clusters in each hemisphere. The hemisphere with the lower number of clusters should contain the $\tau\bar{\tau}$ candidates and is required to have less than eight clusters. The clusters are combined into jets using the algorithm already described but with a y_{cut} value of 0.001 which allows separation of tau pairs down to a mass of 2.9 GeV. We select events in the central region to enhance the signal which has a $\sin^2\Theta$ distribution (fig. 4). the summary of the remaining cuts is:

(4) $N_{\text{cluster}} < 8$ in the tau hemisphere ,

(5) exactly two jets with $y_{\text{cut}} = 0.001$
in the tau hemisphere ,

(6) $\cos\Theta_{\text{thrust}} < 0.7$,

(7) $0.64 < \cos\Theta_{\tau\tau} < 0.98$ for $4 < m_{h^0} < 12$ GeV ,
$0.4 < \cos\Theta_{\tau\tau} < 0.88$ for $12 < m_{h^0} < 22$ GeV ,
$0.1 < \cos\Theta_{\tau\tau} < 0.6$ for $22 < m_{h^0} < 30$ GeV ,

(8) $0.95 < \text{Thrust} < 0.99$ for $4 < m_{h^0} < 12$ GeV ,
$0.91 < \text{Thrust} < 0.96$ for $12 < m_{h^0} < 22$ GeV ,
$0.84 < \text{Thrust} < 0.92$ for $22 < m_{h^0} < 30$ GeV ,

(9) exactly one charged track reconstructed in the central vertex chamber in the direction of each reconstructed tau,

where $\Theta_{\tau\tau}$ is the angle between the reconstructed taus. The overall acceptance for cuts 1 to 9 varies in the range of 6% to 11% depending on the Higgs masses. Background contributions are estimated by

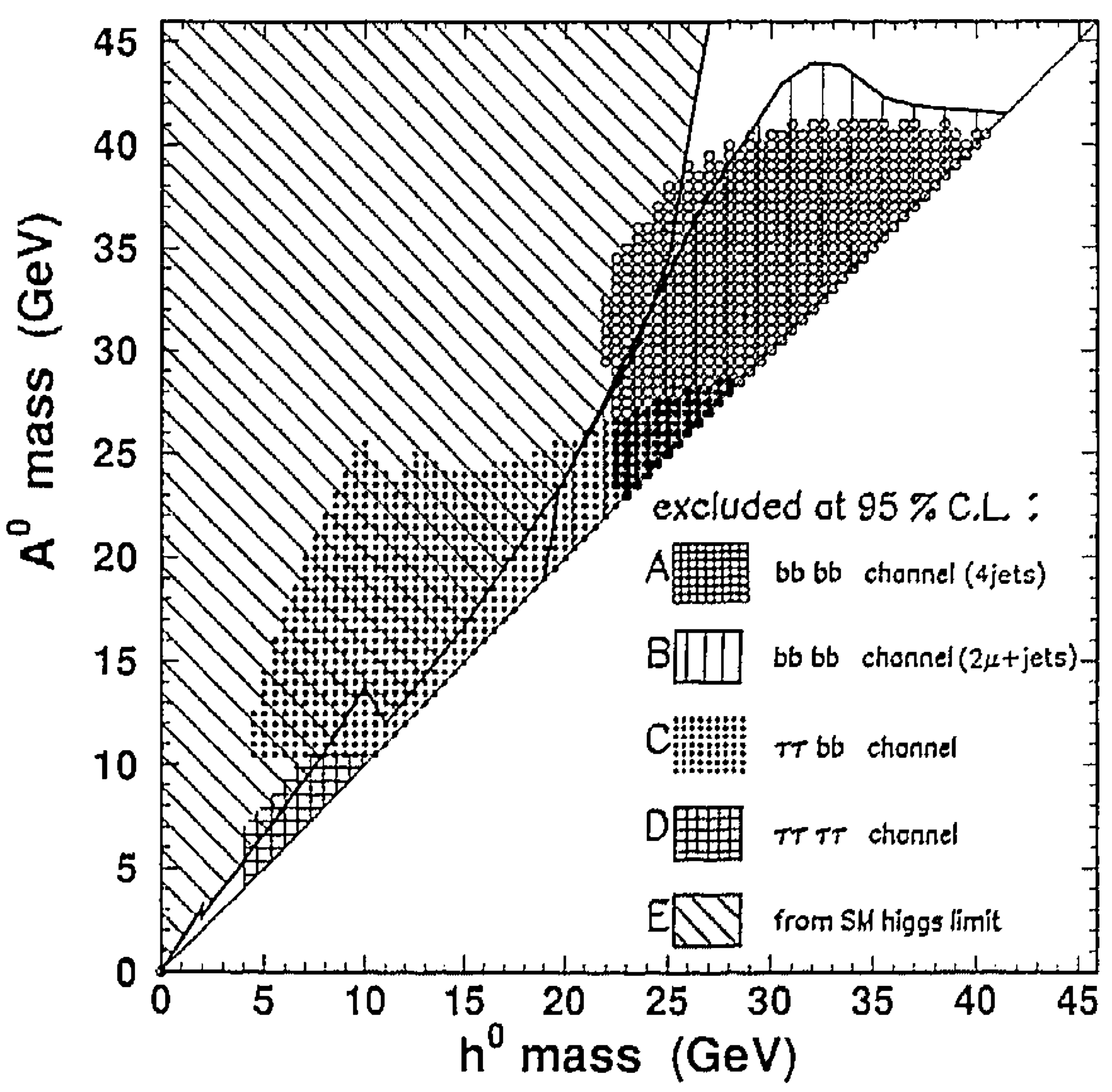

Fig. 3. Exclusion plot for the Higgs masses in the MSSM searches in the mass parameter space (m_{h^0}, m_{A^0}) at 95% CL. The MSSM constrains the search area to $m_{A^0} > m_{h^0}$. Region A is the excluded area from the $h^0A^0 \to b\bar{b}b\bar{b}$ search in the hadronic data sample. Region B is excluded from the $h^0A^0 \to b\bar{b}b\bar{b}$ search in the dimuon data. Region C is excluded from the $h^0A^0 \to \tau\bar{\tau}b\bar{b}$ search. Region D is the excluded area from the $h^0A^0 \to \tau\bar{\tau}\tau\bar{\tau}$ search. Region E is excluded from the inferred limit from the standard model Higgs search. For all decay channels, we assume $\tan\beta > 1$.

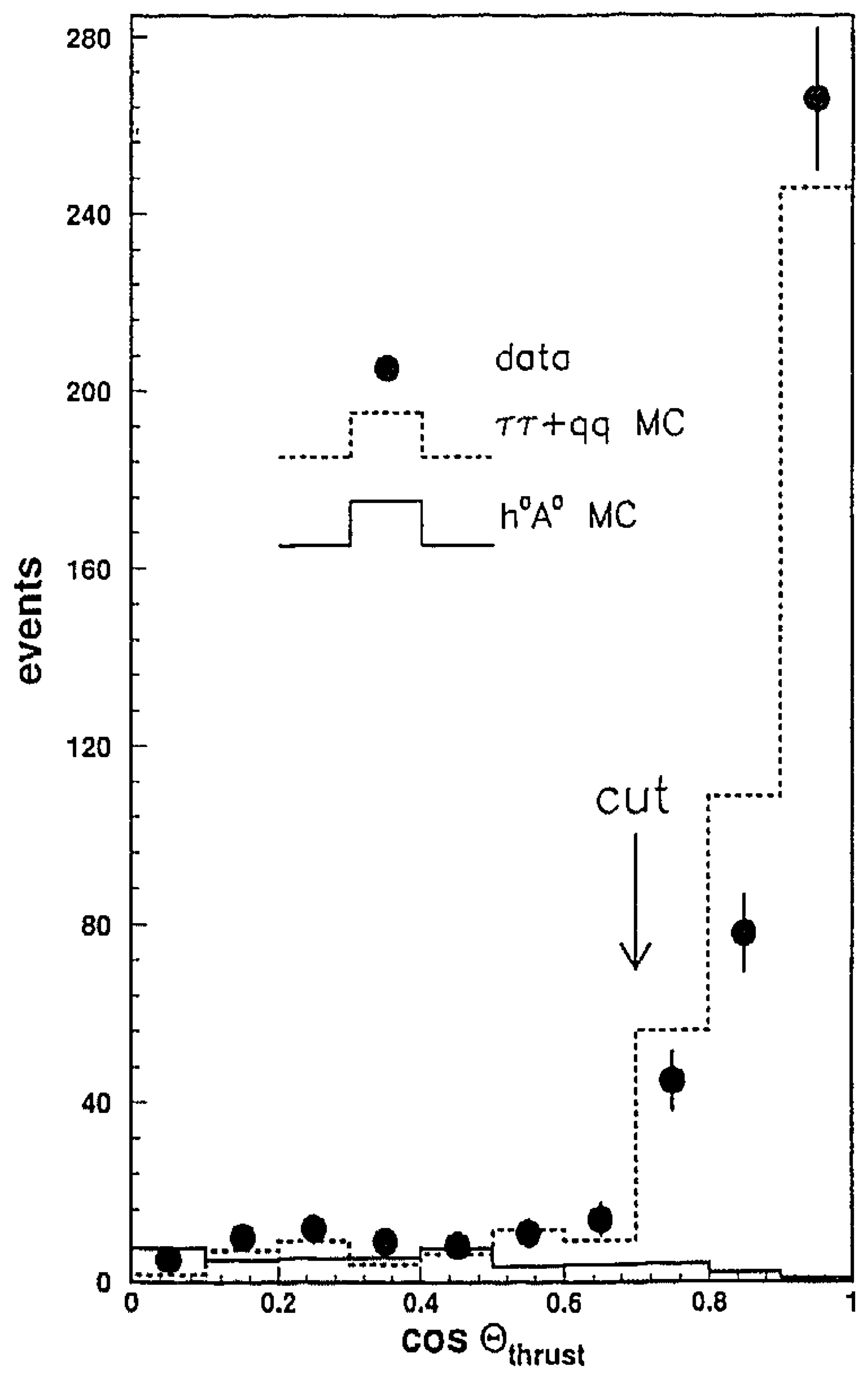

Fig. 4. $\cos\Theta_{thrust}$ for data, $q\bar{q}$ simulation and signal simulation in the $h^0A^0 \to \tau\bar{\tau}b\bar{b}$ search. The peak in the data and in the $q\bar{q}$ simulation is due to the $E_{vis} < 80$ GeV cut, which enhances the rate of events losing energy along the beam direction. Less than eight clusters in the tau hemisphere leading to exactly two jets is required.

simulating 68 K $e^+e^- \to$ hadrons events, and by using the KORALZ generator [24] for simulating 5 K $\tau\bar{\tau}$ events. None of these MC events and none of the data events pass all cuts. A combined statistical and systematic error of 14% has been calculated. The corresponding excluded mass region is shown as area C in fig. 3.

6. Search for $h^0A^0 \to \tau\bar{\tau}\tau\bar{\tau}$

The signatures of four taus are low visible energy, a 4-jet topology with low cluster multiplicity, and events preferentially perpendicular to the beam axis due to the $\sin^2\Theta$ distribution of the production angle. For this analysis we restrict the (m_{h^0}, m_{A^0}) parameter space to the area of a large branching ratio for the production of four taus in the final state. The m_{h^0} range begins at the $\tau\bar{\tau}$ threshold at about 4 GeV and ends at about 11 GeV where the $b\bar{b}$ decays channel starts to dominate. The trigger efficiency for accepted events of this type exceeds 99%. The following cuts are applied:

(1) $40\ \text{GeV} < E_{vis} < 60\ \text{GeV}$,

(2) $\frac{|E_{\parallel}|}{E_{vis}} < 0.50$, $\frac{E_{\perp}}{E_{vis}} < 0.50$,

(3) $12 \leqslant N_{clusters} \leqslant 22$,

(4) $N_{jet} = 4$ for jet resolution parameter $y_{cut} = 0.001$,

(5) $E_{jet} > 2$ GeV,

(6) $\cos\Theta_{thrust} < 0.3$,

In the region $4\ \text{GeV} \leqslant m_{h^0} \leqslant m_{A^0} \leqslant 11$ GeV the expected signal after all cuts is typically more than twelve events. One data event survives the cuts. This is in agreement with the expected number of background events from $Z^0 \to$ hadrons and $Z^0 \to \tau\bar{\tau}$ leading to the exclusion contour D as shown in fig. 3, after taking into account statistical and systematic errors of 12%.

7. Limits from the standard model Higgs search

The expected numbers of standard model Higgs events which would have been detected by L3 has been reported elsewhere [14,15]. Setting $m_{h^0} = m_{H^0_{SM}}$ in eqs. (3) and (4), we can calculate a corresponding lower limit on m_{A^0} at the 95% confidence level, if corrections for the somewhat different MSSM Higgs decay branching ratios are made. For Higgs masses larger than 11 GeV the $b\bar{b}$ decay channel dominates which results in the same detection efficiency for the standard model Higgs search [14] and the MSSM Higgs search.

Below 11 GeV the $\tau\bar{\tau}$ decay channel starts to dominate. In our standard model Higgs search, the acceptance is 5% for $h^0 \to \tau\bar{\tau}$ and 36% for $h^0 \to$ hadrons in the channel $Z^0 \to H^0_{SM} \nu\bar{\nu}$, which leads to a lower detection efficiency for the MSSM compared to the standard model. We use the different acceptances of the modified branching ratios of h^0 to calculate the number of expected events in the MSSM. The corresponding limit on m_{A^0} has been calculated by taking the one Higgs candidate [14] from the standard model search into account.

For Higgs masses in the range $2m_\mu < m_{h^0} < 2$ GeV we can directly translate the number of expected events from the standard model search into a lower limit on m_{A^0}. For masses below $2m_\mu$ the limit on m_{A^0} is computed taking into account the variation of the partial width of the h^0 into electrons and photons. Fig. 3 shows the corresponding excluded area E.

8. Conclusions

We have searched for the pair production of the scalar Higgs boson h^0 and the pseudoscalar Higgs boson A^0. Three decay channels of the h^0A^0 bosons have been studied. The limit inferred from the standard model Higgs search has been combined with the limit from the direct search for the pair produced Higgs bosons. No evidence for the existence of the MSSM Higgs has been found. Nearly the entire mass region up to 41.5 GeV is excluded.

Acknowledgement

We wish to thank CERN for its hospitality and help. We want particularly to express our gratitude to the LEP division: it is their excellent achievements which made this experiment possible. We acknowledge the effort of all engineers and technicians who have participated in the construction and maintenance of this experiment. We acknowledge the support of all the funding agencies which contributed to this experiment.

References

[1] S.L. Glashow, Nucl. Phys. 22 (1961) 579;
S. Weinberg, Phys. Rev. Lett. 19 (1967) 1264;
A. Salam, Elementary particle theory, ed. N. Svartholm (Almquist and Wiksell, Stockholm, 1968) p. 367.
[2] P.W. Higgs, Phys. Lett. 12 (1964) 132; Phys. Rev. Lett. 13 (1964) 508; Phys. Rev. 145 (1966) 1156;
F. Englert and R. Brout, Phys. Rev. Lett. 13 (1964) 321.
[3] Y.A. Golfand and E.P. Likhtman, JETP Lett. 13 (1971) 323;
D.V. Volkhov and V.P. Akulov, Phys. Lett. B 46 (1973) 109;
J. Wess and B. Zumino, Nucl. Phys. B 70 (1974) 39;
P. Fayet and S. Ferrara, Phys. Rep. 32 (1977) 249;
A. Salam and J. Strathdee, Fortschr. Phys. 26 (1978) 57.
[4] E. Witten, Nucl Phys. B 188 (1981) 513;
S. Dimopoulos and G. Georgi, Nucl. Phys. B 193 (1981) 150;
N. Sakai, Z. Phys. C 11 (1981) 153.
[5] H.E. Haber and G.L. Kane, Phys. Rep. 117 (1985) 75;
A. Bartl, W. Majerotto and N. Oshimo, Phys. Lett. B 237 (1990) 229.
[6] ALEPH Collab., D. Decamp et al., Phys. Lett. B 237 (1990) 291;
DELPHI Collab., P. Abreu et al., Phys. Lett. B 245 (1990) 276;
OPAL Collab., M.Z. Akrawy et al., preprint CERN-EP/90-100 (1990);
MARK II Collab., S. Komamiya et al., Phys. Rev. Lett. 64 (1990) 2881.
[7] J.L. Lopez and D.V. Nanopoulos, Phys. Lett. B 245 (1990) 111.

[8] CDF Collab., F. Abe et al., Phys. Rev. Lett. 64 (1990) 142; J. Freeman, in: Proc. 25th Conf. on High energy physics (Singapore, 1990) (World Scientific, Singapore), to be published.
[9] L3 Collaboration, B. Adeva et al., Phys. Lett. B 249 (1990) 341.
[10] J.D. Bjorken, in: Proc. 1976 SLAC Summer Institute on Particle Physics (Stanford, CA, USA), ed. M.C. Zipf (Stanford Linear Accelerator Center, Stanford, CA, 1977) p. 1;
J. Finjord, Phys. Scripta 21 (1980) 143.
[11] P.J. Franzini et al., in: Z. Physics at LEP 1, eds. G. Altarelli, R. Kleiss and C. Verzegnassi, CERN report CERN-89-08, Vol. 2 (CERN, Geneva, 1989) p. 59, and references therein.
[12] S. Dawson, J.F. Gunion, H.E. Haber and G.L. Kane, The physics of the Higgs bosons: Higgs hunter's guide (Addison Wesley, Menlo Park, CA, 1989).
[13] Y. Liu, Z. Phys. C 30 (1986) 631.
[14] L3 Collab., B. Adeva et al., Phys. Lett. B 248 (1990) 203.
[15] L3 Collab., B. Adeva et al., Search for the low mass neutral Higgs boson in Z^0 decay, Phys. Lett. B, to be published.
[16] L3 Collab., B. Adeva et al., Nucl. Instrum. Methods A 289 (1990) 35.
[17] O. Adriani et al., Hadronic calorimetery in the L3 detector, Nucl. Instrum. Methods, to be published,
[18] L3 Collab., B. Adeva et al., Phys. Lett. B 231 (1989) 509; B 237 (1990) 136.
[19] T. Sjöstrand, Comput. Phys. Commun. 39 (1986) 347; in: Z Physics at LEP 1, eds. G. Altarelli, R. Kleiss and C. Verzegnassi, CERN report CERN-89-08, Vol. 3 (CERN, Genua, 1989) p. 143;
T. Sjöstrand and M. Bengtsson, Comput. Phys. Commun. 43 (1987) 367.
[20] GEANT Version 3.13, September, 1989, see R. Brun et al., GEANT 3, CERN DD/EE/84-1 (revised) (September 1987);
to simulate hadronic interactions the program GHEISHA is used, see H. Fesefeldt, RWTH Aachen preprint PITHA 85/02 (1985).
[21] JADE Collab., W. Bartel et al., Z. Phys. C 33 (1986) 23; JADE Collab., S. Bethke et al., Phys. Lett. B 213 (1988) 235.
[22] L3 Collab., B. Adeva et al., Phys. Lett. B 248 (1990) 464.
[23] L3 Collab., B. Adeva et al., Phys. Lett. B 247 (1990) 473.
[24] S. Jadach et al., KORALZ, Proc. Workshop on Z Physics at LEP, eds. G. Altarelli, R. Kleiss and C. Verzegnassi, CERN Report CERN 89-08, Vol. 3 (CERN, Genua, 1989) p. 69, Comput. Phys. Commun., to be published.